Appropriate airmass and solar radiation attenuation parameterisations for southern Africa

H Winkler

Dept. Physics, University of Johannesburg, PO Box 524, Auckland Park, 2006

hwinkler@uj.ac.za

Abstract. Solar power development in South Africa requires accurate knowledge of local solar irradiation characteristics. The amount and spectral distribution of solar irradiation depends on the attenuation of radiation in the atmosphere. This is a function of the solar beam's relative path length through the atmosphere (called airmass), and the aerosol/gas concentration, distribution and physics of light scattering as applied to individual aerosols. Airmass is affected by Earth curvature and refraction, which depend on the atmospheric density profile. Due to the wavelength dependence on attenuation, atmospheric sunlight transmission becomes a complex function of airmass that is generally determined empirically. Most solar irradiation models are based on northern latitude atmospheric profiles, and their applicability to southern African conditions has not been fully tested. This paper describes the evaluation of atmospheric pressure profiles from radiosonde data gathered above De Aar. Light paths are calculated for a range of solar zenith angles and wavelengths. The following are determined and compared with previous work: (i) the characteristic local zenith angle-airmass relationship, and (ii) the locally appropriate integral Rayleigh optical thickness - the airmass-dependent coefficient to the Linke turbidity. In conclusion the paper discusses the implications of these findings for solar energy generation in South Africa.

1. Introduction

The advent of large scale solar energy generation in South Africa has been accompanied by enhanced interest in the accurate parameterisation of solar irradiance.

Even under clear sky conditions, incident sunlight is subjected to interaction with molecules and larger particles in the atmosphere, which dilute the solar beam and scatter rays that are then detected as (generally blue) skylight. The rate of occurrence of scattering events is a function of a number of sometimes interrelated atmospheric parameters, such as the particle nature and concentration, the beam wavelength and the air refractive index.

It also critically depends on the comparative length of a beam's trajectory through the atmosphere, as longer paths imply a greater probability of an encounter with a particle. This comparative atmospheric path length is referred to as the airmass. During times when solar beam obliquity is significant (early morning and late afternoon), the otherwise trivial solar zenith angle vs. airmass relationship increasingly becomes impacted by factors caused by the curvature of the Earth, the air density-height profile and atmospheric refraction effects. In view of the complexity associated with these factors, the zenith angle-airmass relationship is generally defined in terms of empirical formulations obtained from standard northern mid-latitude atmospheric models. This paper will test the applicability of these formulations to South African atmospheric data.

Having achieved that, this study then investigates the relationship under aerosol-free conditions between the broad-band atmospheric transmittance and the airmass, which is characterised by a function referred to as the integral Rayleigh optical thickness. This function is used in solar energy research to determine the fraction of solar light able to transverse the atmosphere. It is also however considered too complex to define analytically with sufficient accuracy. Thus empirical formulations are normally preferred, but these are again based on standard northern hemisphere atmospheric models. This paper evaluates the suitability of these empirical models in southern African conditions.

2. Theory

2.1. Air density

For an ideal gas, the pressure p, volume per mole v and temperature T are related by the expression $pv = RT$, where R is the gas constant. It follows that, in terms of the molar mass μ, the density ρ equals (mass)/(volume) = $\mu/v = \mu p/RT$. For air with a 0.03% per volume fraction of CO_2 that does not contain any water vapour (standard dry air) [1], the molar mass is equal to $\mu_a = 28.9623\times10^{-3}$ kg.mol^{-1}, while for water vapour, $\mu_w = 18.015\times10^{-3}$ kg.mol^{-1} [2].

In order to build in the variable nature of the water vapour contribution to the total molar mass, and to allow for deviation from the ideal gas behaviour, the density equation is modified as follows [2]:

$$\rho = \frac{\mu_a p}{ZRT}\left[1 - X_w\left(1 - \frac{\mu_w}{\mu_a}\right)\right] \tag{1}$$

where X_w is the water vapour fraction (by mole). Z, which is of the order of ~1, is referred to as the compressibility of the air, and is a complex function of both X_w and T that has been parameterised by Ciddor [2].

The water vapour concentration may be determined through measurement of the air pressure, air temperature and dew point temperature Θ. Provided the air saturation point has not been reached, the water vapour partial pressure is given by

$$p_w = \exp\left[1.2378847\times10^{-5}\,\Theta^2 - 1.9121316\times10^{-2}\,\Theta + 33.93711047 + 6343.1645/\Theta\right] \tag{2}$$

where p_w is measured in hPa and Θ is measured in Kelvins [2].

2.2. Zenith angle-airmass relationship

An airmass of $m = 1$ is defined as the equivalent atmosphere traversed by a beam of sunlight when the Sun is directly overhead, i.e. when the angle the direct solar beam makes with the vertical (referred to as the zenith angle ζ) equals zero. Note that in this paper we consider $m = 1$ to be the atmosphere above the site (sometimes referred to as relative airmass), whereas the term is often used in the literature to refer to the atmosphere above sea level (also called absolute airmass).

If one neglects Earth curvature and refraction, the airmass would simply be $m = \sec\zeta$. But when these are considered, the expression for airmass becomes substantially more complex. It has been shown in some of the original studies in this field (see [3] and references quoted therein), using geometric arguments and the refraction law, that the airmass of a beam reaching the surface at a point at a distance r to the centre of the Earth equates to

$$m = \left[\int_0^\infty \rho(h)dh\right]^{-1} \times \int_0^\infty \rho(h)\left(1 - \frac{n(0)^2 r^2}{n(h)^2 (r+h)^2}\sin^2\zeta\right)^{-1/2} dh \tag{3}$$

where h is the height above the surface and $n(h)$ is the refractive index of the atmosphere at height h.

Equation 3 forms the basis for evaluating the airmass as a function of zenith angle, but applying it requires knowledge of the atmospheric density profile, which is location dependent and variable in

time. The most frequently used adaptation of this method is one arising from the 1972 ISO Standard Atmosphere. When applied to 0.7 μm light, the resulting relation is well-fitted by the expression [4]

$$m = \left[\cos\zeta + 0.50572 \times (96.07992° - \zeta)^{-1.6364}\right]^{-1} \quad (\zeta \text{ in degrees}) \tag{4}$$

2.3. The refractive index of air

To quantify the atmosphere's refractive index I use the equations and coefficients determined by Ciddor [2]. Assuming that the CO_2 concentration in the atmosphere is 300 ppm, under standard temperature and pressure (STP: 1013.25 hPa, 15°C), the refractive index of dry air becomes

$$n_{as} - 1 = \frac{0.05791641}{238.0185 - \lambda^{-2}} + \frac{0.00167904}{57.362 - \lambda^{-2}}$$

where the wavelength λ is in μm.

For water vapour, again at STP, the refractive index is

$$(n_{ws} - 1) \times 10^8 = 1.022 \times \left(295.235 + 2.6422\lambda^{-2} - 0.032380\lambda^{-4} + 0.004028\lambda^{-6}\right) .$$

Thus the STP refractive index of dry air at 0.7 μm would be n_{as}(0.7 μm) = 1.00027578, and for water vapour at the same wavelength, n_{ws}(0.7 μm) = 1.00000307. Using the combination formula in Ciddor [2], and after determining the local density of dry air (ρ_a) and water vapour (ρ_w) with equation 1, we obtain

$$n - 1 = \frac{\rho_a}{1.225382}(n_{as} - 1) + \frac{\rho_w}{0.00985938}(n_{ws} - 1) \ , \tag{5}$$

2.4. The integral Rayleigh optical thickness

When traversing the atmosphere, a monochromatic light beam is attenuated according to the relation

$$F(\lambda) = F_0(\lambda)\exp\left(-\tau(\lambda)m\right) , \tag{6}$$

where F is the solar flux per unit wavelength detected at the site, F_0 is the solar flux at the top of the atmosphere and τ is called the optical depth (see e.g. [5]).

Unfortunately one usually does not have the luxury to be able to monitor the spectral development of sunlight during the course of a day. Solar irradiation is more commonly measured by means of broad-band pyranometers, which record total incident light without spectral information. Despite the complications caused by the distortion of the solar spectrum, it is possible to quantify light losses in the atmosphere using the method developed by Linke [6]. The ground-measured flux integrated over all wavelengths is then related to the equivalent quantity above the atmosphere by the expression

$$\int_0^\infty F(\lambda)d\lambda = \left[\int_0^\infty F_0(\lambda)d\lambda\right]\exp\left(-\Lambda\delta(m_0)m_0\right) , \tag{7}$$

where m_0 = (1013.25 hPa)×m/p and Λ is the Linke turbidity. By definition, Λ = 1 for a dry, aerosol-free atmosphere and increases with growing concentrations of particles and water vapour in the air. δ is referred to as the integral Rayleigh optical thickness, as it defines the beam losses due to Rayleigh scattering alone, whose rate of occurrence in the atmosphere is comparatively stable over time and only significantly depends on height above the ground. As with the case with the zenith angle-airmass relation discussed earlier, δ has in general been quantified empirically, mostly in the form

$$\delta(m_0) = \frac{1}{a_0 + a_1 m_0 + a_2 {m_0}^2 + a_3 {m_0}^3 + a_4 {m_0}^4} \ . \tag{8}$$

Different sets of coefficients a_i have been proposed in the literature [7-9], with the most often applied ones in recent years being $\{a_0, a_1, a_2, a_3, a_4\}$ = {6.6296, 1.7513, –0.1202, 0.0065, –0.00013} [10].

3. Data description and results

3.1. Site characteristics and selection of solar irradiation 'golden days'

The South African Weather Services meteorological station at De Aar is located at 24.00E, 30.67S at a height of 1287 m above sea level, corresponding to a distance to the Earth's centre of 6373.895 km [11]. Conditions there are typical of the South African central and western interior. It was designated as a site of the international Baseline Solar Radiation Network (BSRN), and consequently extensive solar irradiation measurements took place here between 2000 and 2007.

In addition, from August 2000 to early 2001 the site also hosted a programme to measure solar irradiance through five narrow wavelength bands by means of sunphotometry [5]. This research identified several cloud-free days during which atmospheric aerosol concentrations were very low. These are here referred to as 'golden days', and the total optical depths determined for two bands unaffected by ozone, water vapour or other molecular absorption are listed in table 1.

Table 1. List of 'golden days' selected and optical depths recorded on those days

Day (2000)	4 Aug	5 Aug	6 Aug	12 Aug	13 Aug	14 Aug	22 Aug	9 Nov	14 Nov	20 Nov	21 Nov
τ(0.415 μm)	0.280	0.277	0.275	0.286	0.270	0.274	0.284	0.302	0.292	0.290	0.296
τ(0.868 μm)	0.014	0.012	0.008	0.020	0.005	0.010	0.016	0.030	0.028	0.022	0.028

3.2. Radiosonde data

In addition to solar irradiation measurements, radiosondes were regularly launched from the De Aar station, which measured the atmospheric pressure p, temperature T and dew point temperature Θ as a function of height h above sea level as part of the BSRN data set [12].

During the golden days the radiosondes were released at noon and captured data at 10 s intervals up to altitudes of at least 24 km. The averaged pressure and temperature profiles are plotted in figure 1.

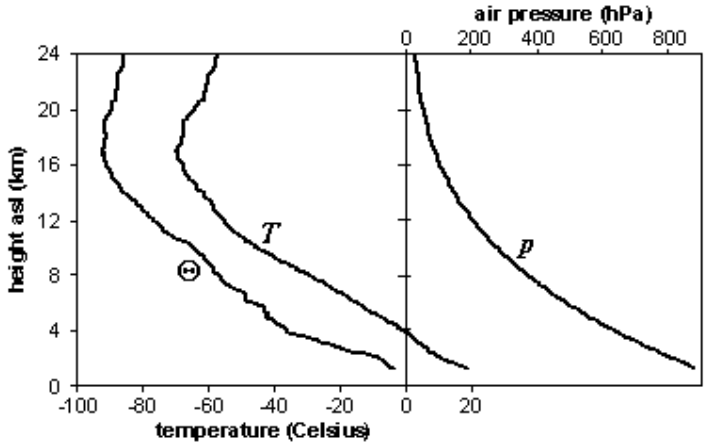

Figure 1. Average golden day atmospheric pressure (p), temperature (T) and dew point temperature (Θ).

3.3. The regional zenith angle-airmass relationship

The recordings were re-binned into 25 m layers within the nominal (0-11 km above sea level (asl)) troposphere and 50 m layers in the nominal stratosphere (> 11 km asl) up to 24 km asl, and averaged over the eleven golden days. Site representative dry air and water vapour densities were then found for each layer with equations 1 and 2, and the layer's refractive index was calculated with equation 5. This was then followed by a numerical integration of equation 3 (in 25 m steps below 11 km and 50 m steps above 11 km), for cos ζ ranging from 0 to 1 in steps of 0.01. The resulting table of m vs. ζ was then fitted by a function $m(\zeta)$ of the same general form as equation 4. The best fit is given below.

$$m = \left[\cos\zeta + 0.49958 \times (95.765° - \zeta)^{-1.6783}\right]^{-1} \quad (9)$$

3.4. The regional integral Rayleigh optical thickness

Although the range of integration in equation 7 extends over the complete wavelength spectrum, the shape of the solar spectrum, as well as the atmosphere's opacity to ultraviolet radiation and part of the infrared, suggest that this may be narrowed without significant loss of accuracy. In line with a previous study [7], the wavelength interval chosen was 0.342-2.348 μm.

As with the refractive index, airmass is also weakly affected by the light wavelength. The procedure lined out in section 2.3 was repeated for the blue 0.415 μm and near-infrared 0.868 μm wavelengths used in the sunphotometer measurements [5], and from that it was confirmed that even when $\zeta \to 90°$, the difference between the blue and near-infrared beam airmass is less than 0.15%. This justifies using the same airmass for all wavelengths covered by the integral.

The solar spectrum for diverse airmass values was determined using the SMARTS2 model [13]. Several of the input parameters used in this model were deduced from the average of the golden day radiosonde data, such as the total atmospheric water column height (= 0.725 cm) and the ground atmospheric pressure relative to STP (= 0.8665). A sample of these spectra may be viewed in figure 2.

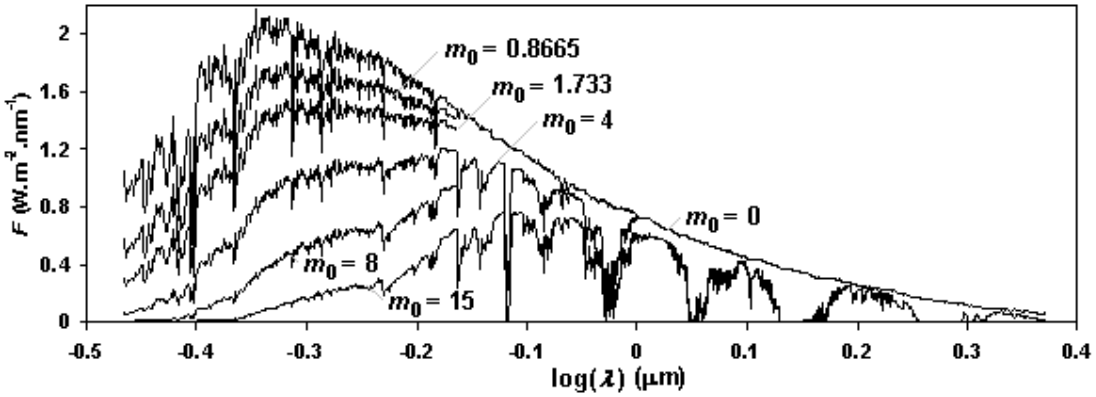

Figure 2. SMARTS2 generated solar spectra in conditions experienced during the golden days for a range of airmass values. Some curves were truncated to avoid cluttering in the diagram.

The average aerosol optical depth for the golden days was determined from the values in table 1 as follows. There are no molecular absorption features in the 415 μm and 868 μm bands, meaning that the average optical depths for these bands, $\tau_{average}$(415 μm) = 0.2842 and $\tau_{average}$(868 μm) = 0.0175, are related by $\tau \propto \lambda^{-\alpha}$ laws, with $\alpha \sim 4$ for Rayleigh scattering and $\alpha \sim 1.3$ for typical aerosols, i.e.

$$\tau(\lambda) = \tau_{Rayleigh}(\lambda) + \tau_{aerosol}(\lambda) \cong \beta_R \lambda^{-4} + \beta_{aer} \lambda^{-1.3} \ , \quad (9)$$

This allows us to calculate that β_{aer}, a further SMARTS2 model input parameter [13], equals 2.55×10^{-3}. The small size of β_{aer} also confirms the very low aerosol concentrations during the golden days ($\tau_{Rayleigh} \sim 3\tau_{aerosol}$). The average golden day Linke turbidity is estimated to be $\Lambda = 2.48$ based on the integrated (0.342-2.348 μm) flux of fully- and just Rayleigh-corrected SMARTS2 spectra at $m_0 = 1$.

Numerical integrations of fluxes over the wavelength intervals (A) 0.342-2.348 μm and (B) 0.35-1.1 μm were performed for a wide range of airmasses (including for $m_0 = 0$, which yielded the integral of F_0). The results were applied to equation 7, with $\Lambda = 2.48$ for case (A) and with $\Lambda = 1.47$ found to be appropriate for the smaller case (B) range. This yielded the set of (m_0, δ^{-1}) points given in table 2.

Table 2. Inverses of the calculated integral Rayleigh optical thicknesses for the (A) 0.342-2.348 μm and (B) 0.35-1.1 μm ranges. m_0 = 0.866, 1.733 and 2.6 correspond to m = 1, 2 and 3 at De Aar.

m_0	0.5	0.866	1	1.733	2	2.6	4	6	8	10	15
$\delta(m_0)^{-1}$ (A)	10.07	12.26	12.86	15.32	16.01	17.34	19.84	22.76	25.34	27.76	33.49
$\delta(m_0)^{-1}$ (B)	9.41	9.99	10.15	10.84	11.05	11.48	12.38	13.54	14.64	15.70	18.27

The values in table 2 were fitted by means of polynomials to determine the a_i coefficients in equation 8. An adequate fit was obtained with an order 3 polynomial with coefficients

$\{a_0,a_1,a_2,a_3\} = \{9.071,3.836,–0.310,0.0109\}$ for 0.342-2.348 μm, and

$\{a_0,a_1,a_2,a_3\} = \{9.089,1.050,–0.0611,0.00213\}$ for 0.35-1.1 μm.

4. Discussion

The revised zenith angle-airmass relationship developed in this paper agrees very closely with the widely used Kasten and Young [4] formulation, confirming its general validity in southern African conditions. The relationship derived in this work and defined by equation 9 is however viewed more accurate in local conditions, as it was specifically obtained from data over a site at altitude and with general conditions typical of the southern African interior.

The integral Rayleigh optical depth function derived for the 0.342-2.348 μm does not match the ones found in previous studies. This is likely to be the result of the strong dependence of atmospheric infrared light transmission on molecular concentrations, especially water vapour, and the way the molecular absorption was parameterised in the different studies. That is one of the major weaknesses in the Linke formulation, which in its original form aimed to merely quantify the degree of turbidity relative to the 'clear' sky solar beam (i.e. not just the Rayleigh-corrected solar beam). To circumvent the above pitfalls, a $\delta(m_0)$ formulation was developed for the narrower 0.35-1.1 μm interval, which in addition corresponds to the approximate sensitivity range of photovoltaic panels and meteorological solar irradiation measuring equipment. It is proposed that this formulation be preferred in that context.

Acknowledgements - This study used radiosonde data collected at the De Aar station of the Baseline Surface Radiation Network (BSRN) of the World Radiation Monitoring Centre. The author thanks the late Danie Esterhuyse for his effort in establishing and maintaining the De Aar BSRN site.

References

[1] Bucholtz A 1995 *Applied Optics* **34** 2765
[2] Ciddor P E 1996 *Applied Optics* **35** 1566
[3] Kasten F 1965 *Theoretical and Applied Climatology* **14** 206
[4] Kasten F and Young A T 1989 *Applied Optics* **28** 4735
[5] Winkler H, Formenti P, Esterhuyse D J, Swap R J, Helas G, Annegarn H J and Andreae M O 2008 *Atmospheric Environment* **42** 5569
[6] Linke F 1922 *Beitr. Phys. fr. Atmos.* **10** 91
[7] Kasten F 1980 *Meteor. Runds.* **33** 124
[8] Louche A, Pery G and Iqbal M 1986 *Solar Energy* **37** 393
[9] Grenier J C, De La Casiniere A and Cabot T 1994 *Solar Energy* **52** 303
[10] Kasten F 1996 *Solar Energy* **56** 239
[11] International Civil Aviation Organisation 1998 *WGS 84 Implementation Manual* version 2.4 http://www2.icao.int/en/pbn/Pages/Documentation
[12] Esterhuyse D 2007 *Baseline Surface Radiation Network (BSRN)*, http://bsrn.awi.de doi:10.1594/PANGAEA.674112-5
[13] Gueymard C 1995 *SMARTS2, A simple Model of the Atmospheric Radiative Transfer of Sunshine*, Florida Solar Energy Centre, https://securedb.fsec.ucf.edu/pub